ORIGINAL ARTICLE

Hydrogeochemical mechanisms and recharge mode of the aquifers under semiarid climate from Morocco

Mohammed Bahir[1] · Driss Ouazar[2] · Salah Ouhamdouch[1]

Abstract

Comprehensive investigations of groundwater were performed in the Ouazzi Wadi area, north part of Essaouira basin, Western Morocco. In the present investigation, hydrogeochemical data together with environmental stable (^{18}O, ^2H, ^{13}C) and radioactive (^3H and ^{14}C) were used to get an insight into the processes controlling groundwater mineralization and their recharge modes. Hydrogeochemical approach revealed that the observed groundwater mineralization is linked to (1) dissolution phenomenon of evaporitics minerals (halite, gypsum, and anhydrite) and of carbonates minerals (dolomite), (2) cations exchange processes, and (3) marine effect. Groundwater quality for drinking purpose has been evaluated and compared to WHO standards; the obtained result shows that the consumption of groundwater in the study area requires a treatment before use as drinking water. As for irrigation purpose, using USSL and Wilcox diagram, groundwater remains suitable for plants supporting high salinity. Data inferred from isotopic approach indicated that (1) the groundwater samples are of a meteoric origin and the recharge of the aquifer is assured by direct infiltration of precipitations without notable evaporation, (2) the recharge of aquifers is assured at the Sebt Kourimat region, near the samples 7, 8, and 9, where the high tritium contents are observed, (3) the age evaluations using radioisotope techniques vary between actual age and Pleistocene.

Keywords Essaouira basin · Hydrogeochemistry · Isotopes · Groundwater · Semiarid condition

Introduction

In view of surface water scarcity in Saharan, arid and semi-arid zones, groundwater remains the main source of water supply to meet domestic, agricultural, and industrial needs. During the last decades, this resource has experienced a qualitative and quantitative degradation due to the overexploitation and the drought episodes recurrence (Bahir et al. 2001, 2016; Ouhamdouch et al. 2016a, b; Re et al. 2013).

In the most coastal area, the groundwater is the main source of freshwater supply and is much exploited to respond to human demands. The high salinization and the pollution in groundwater systems from these areas are generally caused by the effects of seawater intrusion and also mostly ascribed to anthropogenic activities such as domestic wastes, agriculture, and industry, which have negatively affected economic activity and the livelihoods of the people of these areas (Carreira et al. 2014; Qin et al. 2013; Re et al. 2013; Ouhamdouch et al. 2017).

Stable isotopes of oxygen-18 and deuterium are considered to be transported conservatively in shallow aquifer (Vitvar et al. 2005). They are commonly used in combination with groundwater chemistry to identify the flow regimes, groundwater salinity origin, and recharge sources of a groundwater system on local and regional groundwater (Ayadi et al. 2016; Carreira et al. 2014; Clark and Fritz 1997; Edmunds and Tyler 2002; Farid et al. 2013). Indeed, the use of stable isotopes is an important complementary tool that allows the understanding of hydrogeochemical processes that affect water masse, such as mixing and evaporation (Tijani et al. 1996). In this regard, isotopic tracers have been used to highlight the origins of water and recharge mode.
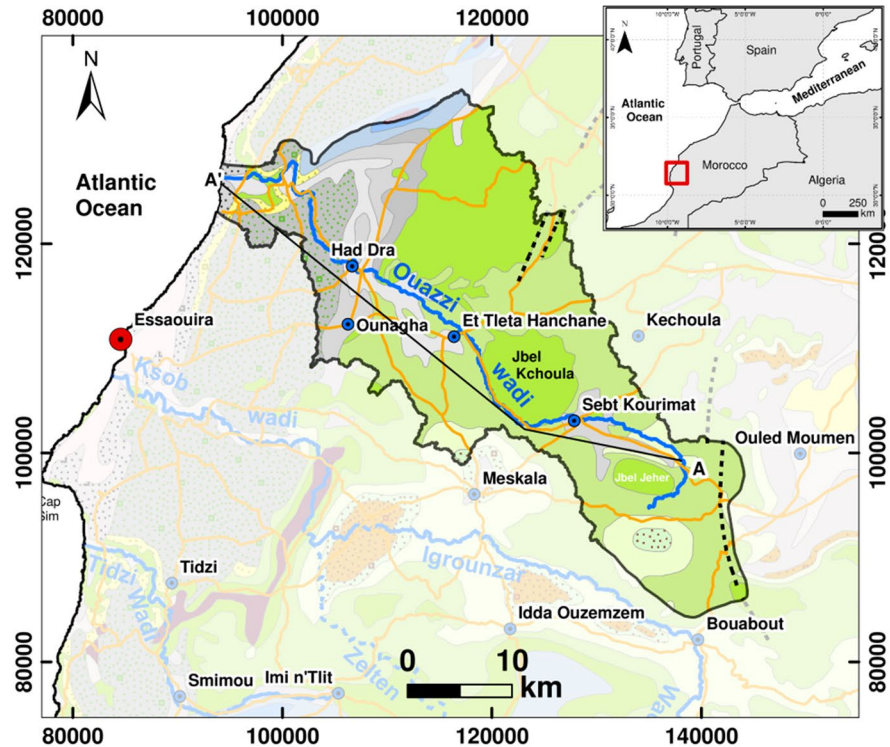
The Ouazzi Wadi basin which was the subject of this study is located in northern part of Essaouira basin, about 20 km northeast of Essaouira city (Fig. 1). Ouazzi Wadi is a
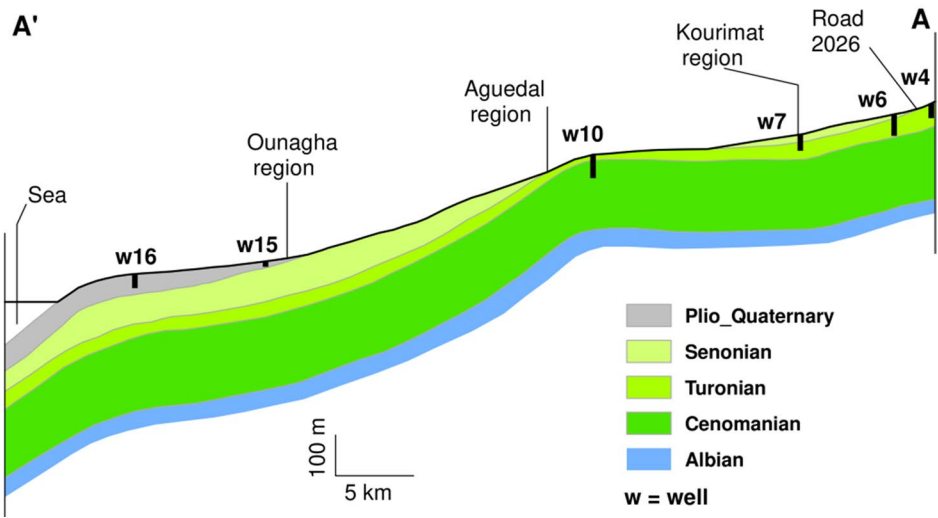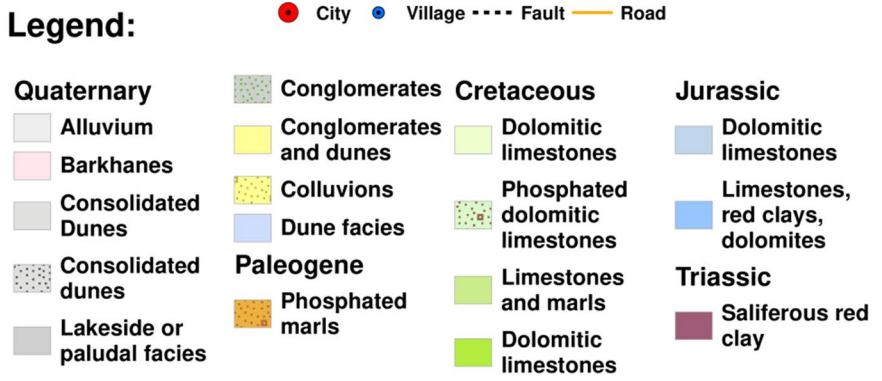
✉ Salah Ouhamdouch
salah.ouhamdouch@edu.uca.ma

1 Laboratoire de Géosciences et Environnement, Département de Géologie, Ecole Normale Supérieure, Université Cadi Ayyad, 40000 Marrakech, Morocco

2 Mohammed VI Polytechnic University, Hay My Rachid, 43150 Ben Guerir, Morocco

Fig. 1 Geographic location, geological map, and cross section of the study area

Legend:

Quaternary
- Alluvium
- Barkhanes
- Consolidated Dunes
- Consolidated dunes
- Lakeside or paludal facies
- Conglomerates
- Conglomerates and dunes
- Colluvions
- Dune facies

Paleogene
- Phosphated marls

Cretaceous
- Dolomitic limestones
- Phosphated dolomitic limestones
- Limestones and marls
- Dolomitic limestones

Jurassic
- Dolomitic limestones
- Limestones, red clays, dolomites

Triassic
- Saliferous red clay

● City   ● Village   ---- Fault   — Road

- Plio_Quaternary
- Senonian
- Turonian
- Cenomanian
- Albian

w = well

typical example of a semiarid climate region where groundwater resources are intensively exploited for human needs as a result of agricultural and demographic development.

Several studies have been realized in the Essaouira basin having partially identified and characterized some of the main mechanisms causing degradation of water quality in some coastal areas of this region, based on the application of geochemical and isotopic approaches (Bahir et al. 2000, 2001; Ouhamdouch et al. 2017, 2018). These studies have demonstrated that: (1) the groundwater recharge in Essaouira basin is supported by water runoff and precipitation; (2) important contribution of water–rock interaction in groundwater mineralization; (3) anthropogenic contamination was also identified.

The main objective of this investigation is to exploit the isotopic and hydrogeochemical tools to highlight processes controlling the groundwater mineralization of the Ouazzi Wadi basin on the one hand and to determine their quality for drinking and irrigation purposes on the other hand. This, in turn, can guide future groundwater management plans in the region.

Study area

The Ouazzi Wadi basin is located in the north-eastern part of Essaouira city (Fig. 1). The basin is under semiarid climate with irregular rainfall of about 300 mm year^{-1} and the temperature oscillates about 20 °C (Ouhamdouch and Bahir 2017).

Geomorphologically, the Essaouira basin is less rugged, with a lower relief characterized by low hills and shaped by a sparse hydrographic network. As for the hydrogeological scope, the study area is a sedimentary basin, mainly composed of two main aquifers. The first is the Plio-Quaternary phreatic aquifer (downstream part, to the west) represented by conglomerates, alluviums, colluvium, and sandstones matrix with a primary hydraulic conductivity by porosity (3.2×10^{-2} m^2/s) and a variant thickness of 5–60 m (Bahir et al. 2000). The substratum of this aquifer is formed by the Senonian gray marls, and the Plio-Quaternary can be in direct contact with the Triassic and Cretaceous formations (Lozes 1959). The results of pumping test studies in this aquifer showed that the Plio-Quaternary transmissivity ranged between 4.5×10^{-5} and 6×10^{-2} m^2/s (Mennani 2001).

The second is the Cenomanian-Turonian carbonate aquifer, and it is mainly constituted by limestones and dolomitic–limestones layers. The Cenomanian is the most important for its power, and its thickness can exceed 220 m. It is composed of gray marls, sandy marls, gypsiferous marls, limestones, sandy limestones, and dolomitic limestones (Jalal 2001). At the outcrop, the Turonian is presented by micritic limestones

and dolomites with the abundance of silica. At depth, there is sometimes intercalation of marly beds (Ettachfine 1992). The Turonian also shows lateral variations of facies and power but in less important proportions than the Cenomanian. Pumping tests results carried out in the study area showed that transmissivity ranged between 2.20×10^{-4} m^2/s and 2.7×10^{-1} m^2/s in Sebt Kourimat region and around 9×10^{-3} m^2/s in Ounagha region (Bahir et al. 2008). The dispersion of transmissivity values comes from the large heterogeneity of lithological facies and the quantitative and qualitative variations of fracturing. This aquifer is exploited by the rural population for drinking water supply and in a lesser extent to agricultural (Bahir et al. 2000). The geological structure of this sedimentary basin is marked by a succession of anticlines and synclines, affected by folded structures and deep faults under the influence of Atlas tectonic and Triassic salt diapers dynamics.

The piezometric map shows that groundwater flows mainly from SE to the NW in upstream and from E to W in downstream, along with the major axis of Ouazzi Wadi (Fig. 2). The natural discharge area of the aquifer is the Atlantic Ocean.

Sampling and analytical procedures

Physico-chemical parameters

A total of 20 water samples have been collected in 2007 from the Plio-Quaternary (downstream) and Cenomanian-Turonian (upstream) aquifers (depth 9.20–170 m) of Ouazzi Wadi basin. The depth of the water table is measured by a piezometric probe (200 m range) (Fig. 2). Temperature, pH, and electric conductivity "EC" were measured on the field. Total alkalinity was determined a few times after collection in the laboratory. Samples have been filtered through 0.45-µm membranes. The filtered samples were collected in polyethylene bottles, which were prewashed with acid and rinsed by sampled well water. The chemical analyses (Ca, Mg, Na, K, Cl, SO$_4$, and NO$_3$) of the waters were performed at the Laboratory at Sciences Faculty of Semlalia of Marrakech (Morocco) by using the ion chromatography.

Saturation index

Calculation of saturation indices for the 20 samples was made using the geochemical modeling software PHREEQC for windows (Parkhurst and Appelo 1999). These indices are calculated according to the formula (1):

$$\text{SI} = \log \frac{\text{IAP}}{K_i} \tag{1}$$

where SI saturation index, IAP ion activity product, and K_i the equilibrium solubility constant.

Fig. 2 Sample location and piezometric map
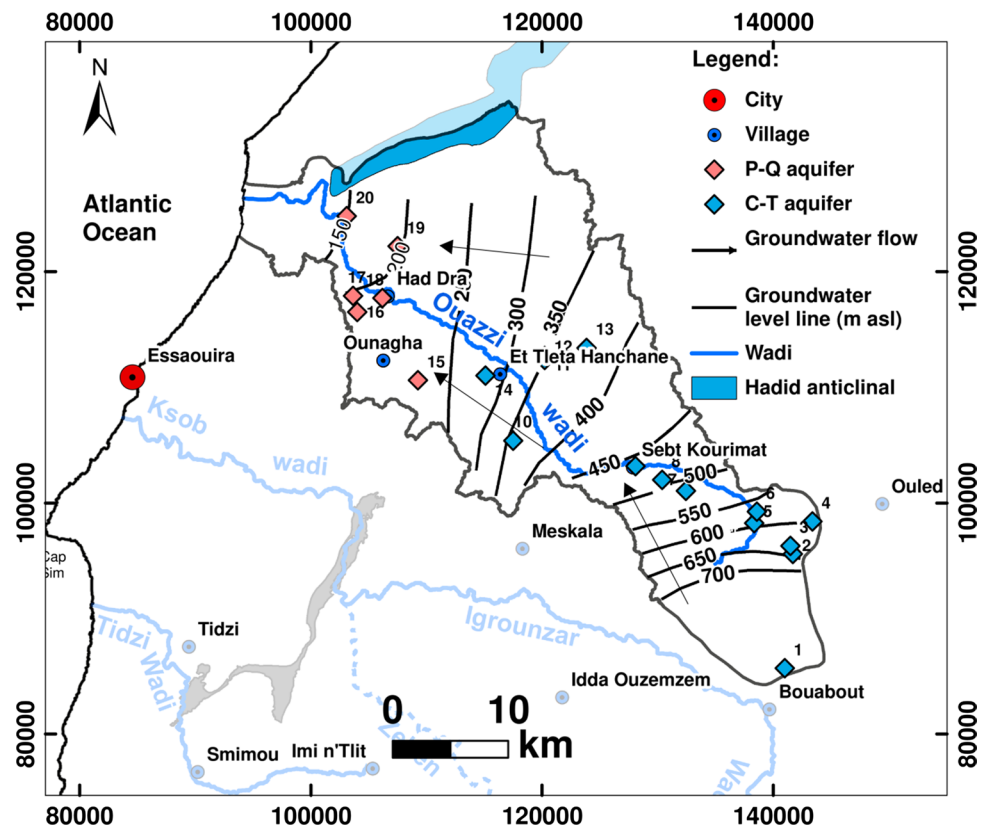
Sodium adsorption ratio (SAR) and sodium percentage (%Na)

SAR is an important parameter to assess the groundwater aptitude for irrigation. It is easily measurable by applying the formula (2) (USSL 1954):

$$SAR = \frac{Na}{\sqrt{\frac{Ca+Mg}{2}}} \tag{2}$$

The %Na parameter is a common parameter for assessing the suitability of natural water for irrigation. This parameter is calculated according to the formula (3) (Wilcox 1955):

$$\%Na = \frac{Na \times 100}{Ca + Mg + Na + K} \tag{3}$$

Stable and radioactive isotopes

The δ^2H and $\delta^{18}O$ of the water samples were determined by using mass spectrometry following the methods proposed by Friedman (1953) and by Epstein and Mayeda (1953) for ^2H and ^{18}O, respectively, with a precision of $\pm 1‰$ for δ^2H and $\pm 0.1‰$ for $\delta^{18}O$. The stable isotope data, δ^2H and $\delta^{18}O$, are reported to V-SMOW (Vienna-Standard Mean Ocean Water) in ‰.

The tritium (^3H) content was determined using the electrolytic enrichment followed by liquid scintillation counting method (IAEA 1976; Lucas and Unterweger 2000). The error associated with the ^3H measurements varies with the ^3H concentration in the water sample.

The ^{13}C and ^{14}C determinations were made on the TDIC (Total Dissolved Inorganic Carbon) of groundwater, precipitated in the field as $BaCO_3$ at a pH higher than 9.0. The counting rates of the ^{14}C (benzene) were measured using a liquid scintillation counter. ^{14}C content is expressed in pMC (percentage of Modern Carbon). The ^{13}C values, obtained in the TDIC by mass spectrometry, are reported in ‰ to V-PDB (Vienna–PeeDee Belemnite) standard, with an accuracy of $\pm 0.1‰$.

All the isotopic analyses were performed in the laboratories of IAEA-IHS (International Atomic Energy Agency—Isotope Hydrology Section) in Vienna, Austria.

The results of chemical and isotope analyses are grouped in Tables 1 and 3.

Results and discussion

Hydrogeochemical frameworks

Hydrochemical characterization and water type

A total of 20 groundwater samples were analyzed for physical [pH, T and electrical conductivity (EC)] and chemical

Table 1 Analytical result for physico-chemical and major ions

	Min	Max	Mean	WHO standard (2008)
T (°C)	17.40	26.60	22.29	–
pH	6.65	7.80	7.22	6.5–8.5
EC (μs/cm)	900	3900	2180	1500
Ca (mg/L)	49.30	681.99	215.62	200
Mg (mg/L)	35.23	338.01	138.07	30
Na (mg/L)	43.40	309.15	149.33	200
K (mg/L)	2.10	66.28	12.24	–
Cl (mg/L)	68.45	1201.67	426.15	250
SO_4 (mg/L)	7.74	2392.54	500.51	250
HCO_3 (mg/L)	183.00	457.50	338.34	–
NO_3 (mg/L)	12.87	214.05	73.49	50

(major ions) parameters. The results are summarized in Table 1. The pH of the analyzed samples varies between 6.55 and 7.80, with an average of 7.22. The water of the study area is a hypothermal type with an average of temperature of 22.29 °C. For the EC, it varies from 900 to 3900 μs/cm with an average of 2180 μs/cm. For anions, Cl and HCO_3 are the major anions with average concentrations of 10.91

and 5.62 meq/L, respectively. Table 1 shows that the average SO_4 content is 10.65 meq/L, but, except for two samples with concentrations of 49 meq/L, the average concentration becomes 5.04 meq/L and therefore lower than that of HCO_3. As for cations, the main ions are Ca and Mg with concentrations 10.56 and 11.30 meq/L, respectively.

Piper diagram (1944) is a diagram for grouping samples and providing an idea of groundwater origin. The projection of 20 samples analyzed on the Piper diagram (Fig. 3) shows three water types: Mg–Ca–Cl type, Mg–Ca–HCO_3 type, and SO_4–Ca–Mg water type. The dispersion of the points in the Piper diagram suggests that the groundwater mineralization is of several origins.

The results of the saturation indices obtained using the PHREEQC software (Parkhurst and Appelo 1999) are grouped in Fig. 4. However, the groundwater is undersaturated with respect to the halite, gypsum, and anhydrite. Nevertheless, they show positive saturation index values with respect to calcite and dolomite.

Gibbs diagrams (1970) are used to evaluate the processes responsible for the origin of dissolved chemical elements, such as rock weathering dominance, precipitation dominance, and evaporation dominance (Gibbs 1970). It is widely used and has given satisfactory results (Nagaraju et al. 2014; Li et al. 2015; Krishna et al. 2017). Tracing the correlation

Fig. 3 Piper diagram of groundwater samples. C-T = Cenomanian-Turonian, P-Q = Plio-Quaternary
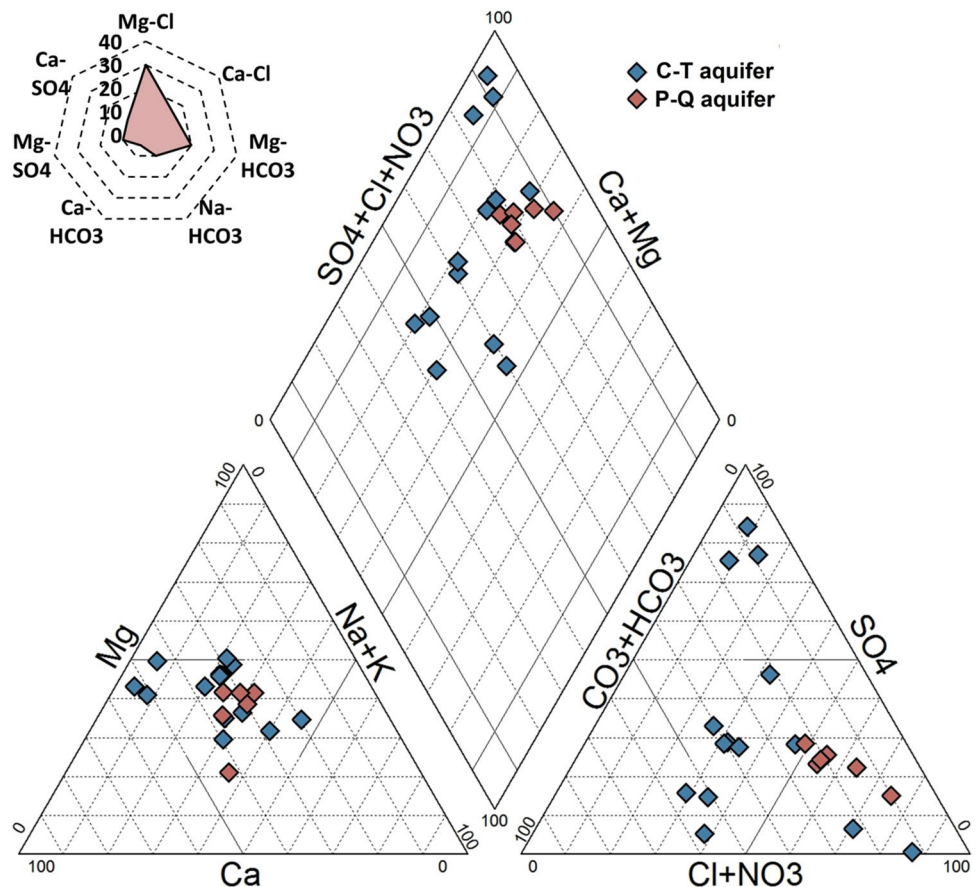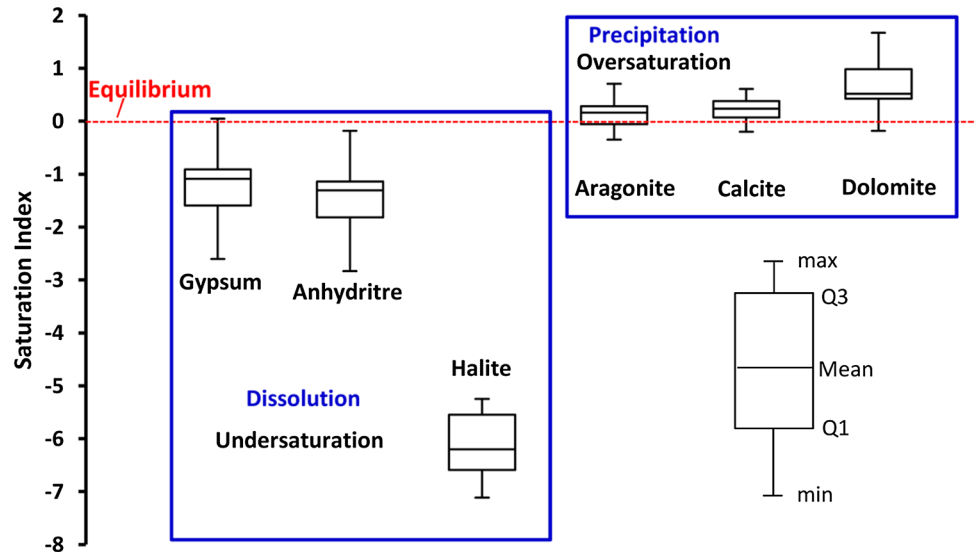
Fig. 4 Saturation indices for several minerals

diagrams of Na/(Na + Ca) versus TDS and Cl/(Cl + HCO₃) versus TDS (Fig. 5) shows that the chemical composition of groundwater is dominated by the evaporation and rock weathering phenomena.

Calculation of the correlation is an important step in revealing the statistical link between two or more variables. As shown in Table 2, the Ca, Mg, and SO_4 ions are positively correlated with TDS. This indicates the contribution of these ions to the mineralization of groundwater.

Ca ion is positively correlated with Mg ion, with a correlation coefficient of 0.91 indicating that these two ions probably have the same origin. Ca–Mg correlation diagram (Fig. 6b) shows that the points are scattered around the dolomite dissolution line (line 1:1). Dolomite dissolution is supported by the negative saturation indices presented by some analyzed points (Fig. 5). For Ca and SO_4, they are positively correlated with a correlation coefficient of 0.91 (Table 2). This suggests that these two ions have the same origin. The diagram of Ca versus SO_4 (Fig. 6c) shows that some points are aligned on the straight line of slope 1, gypsum and anhydrite dissolution line. This

phenomenon is supported by negative saturation indices with respect to gypsum and anhydrite (Fig. 5). Ca excess can be explained by the phenomenon of reverse cation exchange (Fig. 7). While SO_4 excess for some samples perhaps explains the direct Cation Exchange process (Fig. 7). As shown in Table 2, Mg is positively correlated with SO_4. The Mg–SO_4 correlation diagram (Fig. 6d) shows an excess in Mg which can be explained by the reverse cation exchange phenomenon. Table 2 shows a very weak and negative correlation between Ca and HCO₃, suggesting that the dissolution of calcite does not contribute to the groundwater mineralization in the study area. This hypothesis is supported by positive saturation indices with respect to calcite (Fig. 5).

Cl contents are positively correlated with Na contents with a correlation coefficient of 0.80 (Table 2). This suggests that these two ions have the same origin. The Na versus Cl diagram (Fig. 6a) shows that some points are located near the 1:1 line reflecting the participation of halite dissolution in the groundwater mineralization of the study area. This hypothesis is confirmed by negative saturation indices with

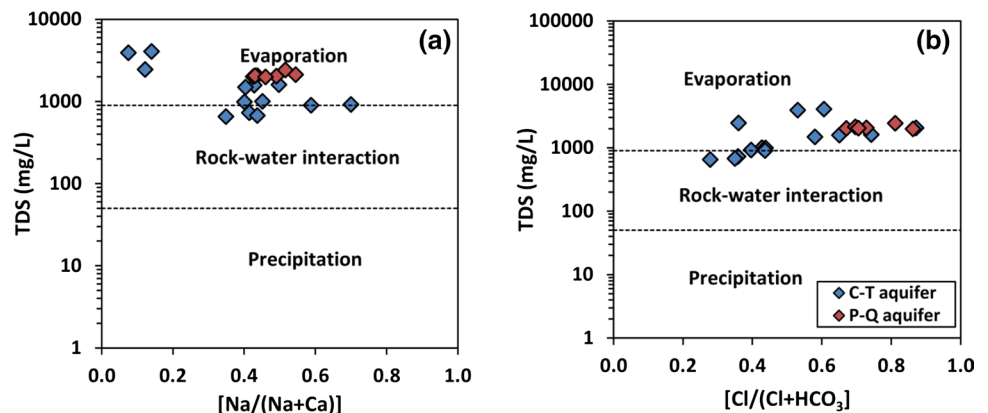**Fig. 5** Gibbs' diagrams. C-T = Cenomanian-Turonian, P-Q = Plio-Quaternary

Table 2 Correlation matrix of the major ions and the TDS for the study area

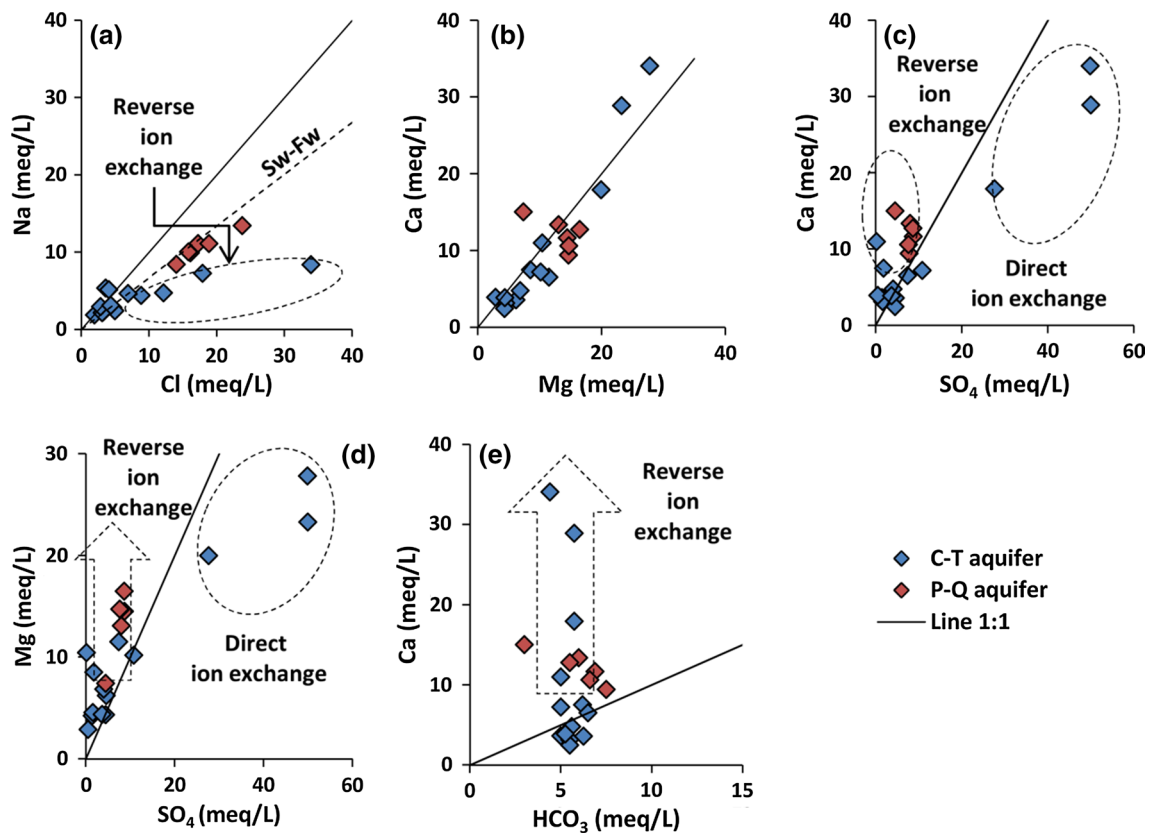| Variables	TDS	Ca	Mg	Na	K	Cl	HCO₃	SO₄
TDS	**1**							
Ca	**0.96**	**1**						
Mg	**0.95**	**0.91**	**1**					
Na	0.24	0.07	0.15	**1**				
K	0.15	0.23	− 0.04	0.31	**1**			
Cl	0.31	0.14	0.19	**0.81**	0.16	**1**		
HCO₃	− 0.04	− 0.22	0.12	0.14	**− 0.66**	0.06	**1**	
SO₄	**0.86**	**0.91**	**0.86**	− 0.23	0.04	− 0.20	− 0.10	**1**

A good correlation is represented in bold

Fig. 6 Correlation diagram **a** Na versus Cl **b** Ca versus Mg **c** Ca versus SO₄ **d** Mg versus SO₄ and **e** Ca versus HCO₃. C-T = Cenomanian-Turonian, P-Q = Plio-Quaternary

respect to halite (Fig. 5). Further points are located below the 1:1 line, suggesting the contribution of other phenomena to the groundwater mineralization in the study area. The Na deficiency can be explained by the excess of Ca and Mg following the base exchange process (Fig. 7). As shown in Fig. 6a, the samples from the Plio-Quaternary aquifer (toward the Atlantic Ocean) are aligned on the right sw–fw. This reflects the marine influence on groundwater mineralization in the study area.

Figure 7b shows that the samples of the Cenomanian-Turonian aquifer are distributed around the 1:1 line, which

indicates the dissolution of carbonate (especially the dolomite) and evaporitic (gypsum and anhydrite) minerals. Samples located above the 1:1 line indicate an excess of Ca and Mg leading to the reverse base exchange phenomenon. To confirm that the cation exchange process contributes to the groundwater mineralization in the study area, we used the correlation diagram $(Ca + Mg - HCO_3 - SO_4)$ versus $(Na + K - Cl)$ (Fig. 7a). This shows that the slope of the correlation line is − 0.71 confirming that ion exchange can be a phenomenon contributing to the groundwater mineralization. The majority of the points are localized toward the
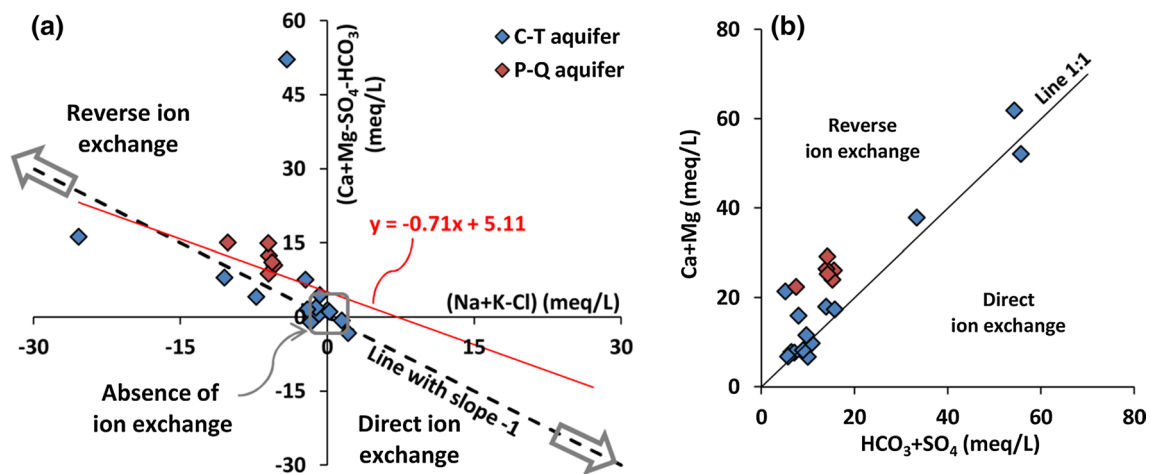
Fig. 7 Correlation diagram **a** $[(Ca+Mg)-(HCO_3+SO_4)]$ versus $[(Na+K)-Cl]$ **b** $(Ca+Mg)$ versus (HCO_3+SO_4). C-T = Cenomanian-Turonian, P-Q = Plio-Quaternary

positive ordinates and toward the negative abscissae; this reflects an enrichment of Ca and Mg with respect to Na following the fixation of Na and release of Ca and Mg by the aquifer matrix. However, according to this diagram, the groundwater mineralization of the study area is controlled by the cation exchange phenomenon that is added to the dissolution process and to the marine influence.

Groundwater quality for drinking purposes

Evaluation of the groundwater quality with drinking purposes was made by comparing the physico-chemical parameters of the analyzed samples with the thresholds set by WHO (2008). The results obtained are grouped in Table 1. With the exception of Na and pH, that present the values lower than the limits fixed by WHO (2008), the electrical conductivity and the rest of the ions have values exceeding the threshold set by WHO (2008). Due to the food nature of the agriculture practiced in the study area, intake by plants and fertilizers is negligible or nonexistent. However, high levels of NO_3 would come from domestic pollutants, as this pollution is a one-off phenomenon. Only the catchment points are polluted, and this pollution originates from the traditional methods of drawing. These result in a significant amount of water flowing around the catchment wells, constituting quasi-permanent pools that are enriched in NO_3 by livestock waste during watering. However, the consumption of groundwater in the study area requires a treatment before use as drinking water.

Groundwater quality for irrigation purposes

SAR is an important parameter to assess groundwater for irrigation purposes. It is widely used in many zones and

has yielded satisfactory results (Al-Ahmadi 2013; Giuseppe et al. 2014; Gowrisankar et al. 2017). In the study area, the samples from the Cenomanian-Turonian aquifer fall into the categories C3S1 and C3S4, while those from the Plio-Quaternary aquifer fall into the category C4S1 (Fig. 8). However, groundwater in the study area remains suitable for plants with high salinity.

As for the %Na parameter, the values calculated in the study area vary between 3.77 and 42.95% (Fig. 9). The projection of the analyzed samples on the %Na versus EC (Fig. 9) diagram shows that the points are in the three categories "Good to Permissible", "Doubtful to Unsuitable", and "Unsuitable". However, groundwater in the study area remains valid for plants with high Na and high salinity.

Isotopic frameworks

The stable isotopes oxygen-18 and deuterium are two essential elements to determine the groundwater origin. They also provide information on processes that may affect water before or during infiltration, such as evaporation phenomenon (Geyh 2000). The use of these elements in combination with physico-chemical parameters makes it possible to decipher the mechanisms controlling groundwater mineralization (Ben Cheikh et al. 2014; IAEA 1981, 1983).

The result of oxygen-18 and deuterium analyses of groundwater samples indicate that the oxygen-18 contents range between −6.20 and −3.82‰, and deuterium contents vary from −38.37 to −20.69‰ (Table 3).

Results from the investigated area are shown in Fig. 10 in relation to the Global Meteoric Water Line (GMWL) $(\delta^2H=8\times\delta^{18}O+10)$ (Craig 1961) and the Local Meteoric Water Line (LMWL) $(\delta^2H=7.55\ \delta^{18}O+9.2)$ (Bahir et al.

Fig. 8 Salinity versus alkalinity hazard in the US salinity diagram. C-T = Cenomanian-Turonian, P-Q = Plio-Quaternary
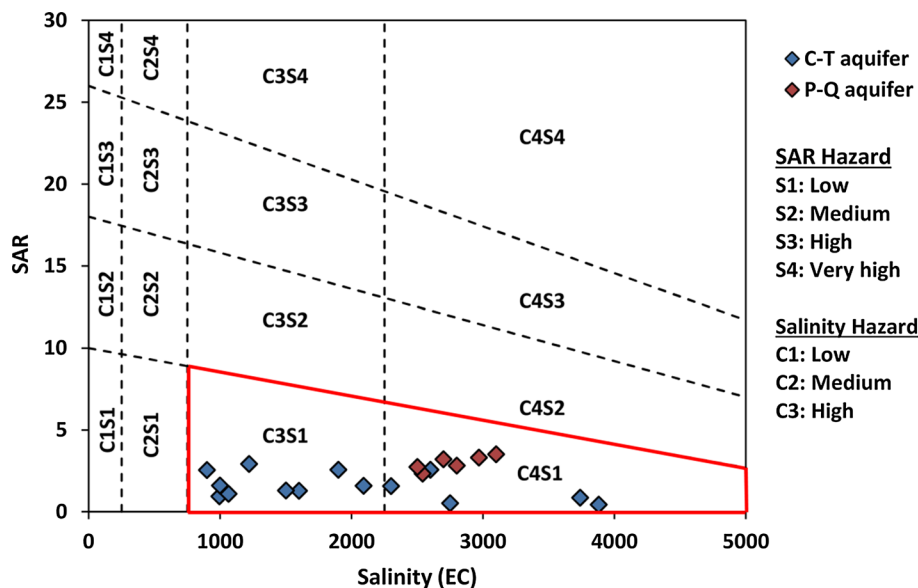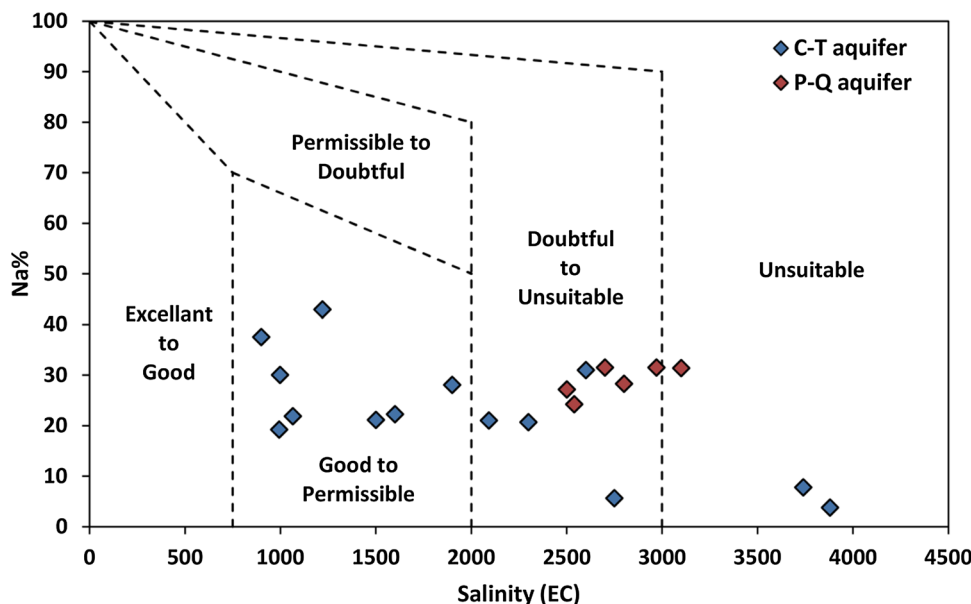

Fig. 9 Suitability of groundwater for irrigation in Wilcox diagram. C-T = Cenomanian-Turonian, P-Q = Plio-Quaternary

2000). The close proximity to the meteoric water lines suggests that the water was of meteoric origin.

All points are placed above the GMWL, reflecting a direct recharge without evaporation.

When the points analyzed for ^2H and ^{18}O draw a line of slope 8 in diagram ^2H versus ^{18}O, it means that these waters are of meteoric origin. Whereas when the slope is less than 8, this reflects evaporation during or/and after the rainfall (Al-Charideh et al. 2009). For the study area, we note that the calculated slope of $^2H/^{18}O$ is 7.76 and 7.40 for the water from the Cenomanian-Turonian and Plio-Quaternary aquifer, respectively. This confirms that recharge of aquifers in the study area is ensured by direct infiltration of rainwater.

Diagram of chloride versus oxygen-18 (Fig. 11a) shows that the chloride concentrations are not correlated with the oxygen-18 contents, and this highlights the importance of the dissolution phenomenon in the study area. In addition, the calculated correlation coefficients between Cl and ^{18}O of samples from the Cenomanian-Turonian and Plio-Quaternary aquifers are $R^2 = 0.045$ and $R^2 = 0.003$, respectively. This suggests that evaporation appears to be a nonsignificant process involved in the groundwater mineralization in the study area.

The tritium is one of the radioactive isotopes used to estimate the water age. However, a recent recharge of such an aquifer may be marked by tritium contents greater than 1, whereas water with tritium content less than 1 is considered

Table 3 Isotopic data of sampled groundwater

Sample	$\delta^{18}O$ ‰ V-SMOW	δ^2H	Tritium (2007) TU	Tritium (2016)	^{14}C % mod.	^{13}C ‰
1	−5.5	−34.3	–	–	–	–
2	−5.6	−34.2	–	–	–	–
3	−5.9	−35.7	–	0.9	86.0	−5.1
4	−5.6	−35.1	0.8	–	22.4	–
5	−5.4	−34.3	0.4	0.4	–	–
6	−5.3	−31.6	2.0	0.8	–	–
7	−5.7	−33.3	1.7	0.0	60.5	−10.8
8	−5.7	−32.7	3.4	1.5	–	–
9	−5.4	−31.4	1.9	0.7	–	–
10	−4.7	−26.6	0.4	–	–	–
11	−5.2	−29.8	–	–	2.2	–
12	−5.3	−29.1	0.2	–	–	–
13	−4.9	−28.9	–	0.2	–	–
14	−5.4	−31.4	1.3	0.2	67.4	−10.4
15	−3.8	−20.7	–	0.6	–	–
16	−6.2	−38.4	–	0.0	59.9	−7.4
17	−4.9	−27.9	–	–	67.7	−9.2
18	−4.7	−24.5	–	0.7	–	–
19	−4.2	−23.7	–	1.0	–	–
20	−4.8	−27.6	0.8	0.7	74.4	−8.4

as water resulting from an age recharge before nuclear tests (Mazor 1991). Tritium activities were measured on samples to establish the groundwater residence time. According to Clark and Fritz (1997), the presence of detectable activities of tritium in groundwater highlights the modern infiltration of rainwater in these aquifers. In fact, tritium values in the study area range from 0.18 to 3.43 TU for the 2007 campaign and from 0.00 to 1.5 TU for the 2016 campaign (Fig. 11b, Table 3). The presence of measurable tritium concentrations

Fig. 10 δ^2H–$\delta^{18}O$ stable isotope diagram of the analyzed groundwater samples. C-T = Cenomanian-Turonian, P-Q = Plio-Quaternary

(> 1 TU) is observed in the Cenomanian-Turonian aquifer of the study area, confirming the presence of recent waters (6, 7, 8, and 9). But, the results of the 2016 campaign show that all the samples, with the exception of sample 8, have very low tritium contents (< 1 TU). This can be explained by the precipitations scarcity that has known the study area in last years. However, the waters sampled in 2016 are the result of a recharge that takes place before the nuclear tests of the 50 s. This reflects a low renewal of aquifers in the study area.

The age estimation of groundwater is an important step toward better management and protection of this resource. An aquifer with water of considerable age means that the renewal rate of this aquifer is low. Nevertheless, a significant turnover rate suggests a recent recharge. ^{14}C radioactive isotope, which has the capacity to date water up to an age of 30,000 years, is the most commonly used element for groundwater dating (Edmunds 2009). A carbonate matrix of such aquifer or even the presence of a carbonate layer in this aquifer makes the dating method of groundwater by ^{14}C very difficult.

A common and straightforward way to estimate the initial ^{14}C activity is by relating the $\delta^{13}C$ content of the DIC in the groundwater to the mixed carbon from carbonate rocks, using carbon from soil CO_2 and a fractionation factor between the different carbonate phases as a function of temperature (Gonfiantini and Zuppi 2003).

Data for water samples from the study area range from −5.12 to −10.82‰. Variations in $\delta^{13}C$ of DIC in this area
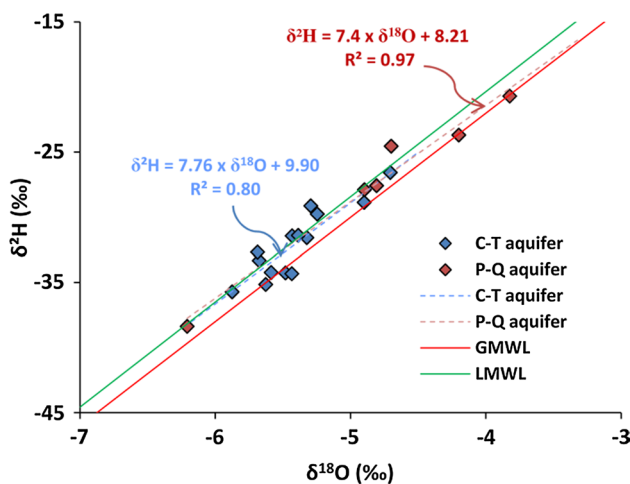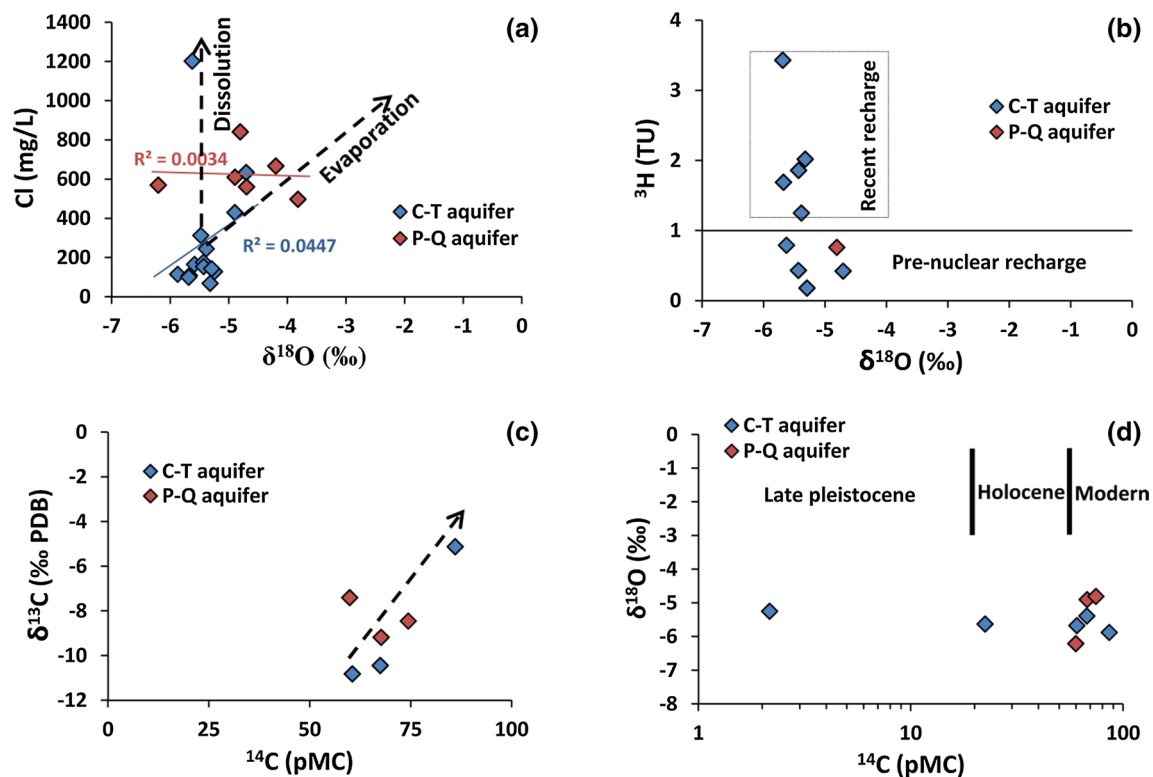
Fig. 11 **a** $\delta^{18}O$ versus Cl diagram, **b** $\delta^{18}O$ versus ^3H, **c** $\delta^{13}C$ versus ^{14}C, **d** $\delta^{18}O$ versus ^{14}C. C-T = Cenomanian-Turonian, P-Q = Plio-Quaternary

are plotted as a function of the ^{14}C activities (Fig. 11c). However, there do not appear to be appreciable trends in $\delta^{13}C$ of DIC within individual hydrochemical zones what may indicate that source waters recharged to the aquifers are similarly influenced by the isotopic composition of carbonate minerals and by the relative abundances of different plants in the recharge areas. However, the increase in ^{14}C activities and ^{13}C enrichment could be explained by the mixing of biogenic CO_2 and carbonate mineral matrix.

The age values for water of the study vary between the actual to 2300 BP. Even if radiocarbon is an indispensable tool in the age tracing of groundwater, results must always be approached with caution. The reliability of results depends strongly on the complexity of the geochemistry of the aquifer. According to the correspondence ^{14}C (%)/infiltration period scaling by several authors in North Africa (Guendouz et al. 2003; Kamel et al. 2008), the ^{18}O content (‰) are plotted against ^{14}C (pMC) for Cenomanian-Turonian and Plio-Quaternary groundwaters in the study area (Fig. 11d). The activities of ^{14}C between 2 and 20 pMC in the analyzed waters correspond to the late Pleistocene recharge period where the climate is wetter and colder than the current. The presence of groundwater with a ^{14}C activity of 20–60 pMC with an average isotopic composition of -5.5‰ versus SMOW for oxygen-18 indicates a relatively newer Holocene recharge. Groundwater with ^{14}C activity above 70 pMC

suggests actual recharge. However, the study area contains both fossil water and recent water. This corroborates the result obtained from relation ^3H versus oxygen-18.

Conclusion

The geological setting of Ouazzi Wadi basin and the flow of Ouazzi Wadi, during rainfall, plays an important role in the geochemical and hydrodynamic characteristics in the studied area. Hydrogeochemistry and isotope hydrology of groundwater in this area have provided useful insights into their origin, mineralization processes, and recharge mechanisms.

Hydrogeochemical approach revealed that the observed groundwater mineralization is linked to (1) dissolution phenomenon of evaporitics minerals (halite, gypsum, and anhydrite) and of carbonates minerals (dolomite), (2) cations exchange processes, and (3) marine effect. Groundwater quality for drinking purpose has been evaluated and the consumption of groundwater in the study area requires a treatment before use as drinking water. As for irrigation purpose, groundwater in the study area remains suitable for plants supporting high salinity.

The stable isotope signatures indicate that the groundwater samples are of a meteoric origin. These tracers reveal the recharge of the aquifer is assured by direct infiltration of

precipitations without notable evaporation. The high tritium contents (^{3}H > 1 TU) are observed at the water points 7, 8 and 9 (near the Sebt Kourimat village = recharge zone of the aquifer) for the 2007 campaign. The comparison of the ^{3}H contents for the same samples from the 2007 and the 2016 cohorts shows a decrease in ^{3}H. This diminution can be explained by the precipitations scarcity that has known the study area in recent years. However, the waters sampled in 2016 are the result of a recharge that takes place before the nuclear tests of the 50 s, reflecting a low renewal of aquifers studied. Age evaluations using radioisotope techniques vary between the actual age to Pleistocene.

However, the scientific results of this study could be exploited for a water management of the area to sustainably develop the exploitation of the resource, taking into accounts its dynamics and renewability.

Compliance with ethical standards

References

Al-Ahmadi ME (2013) Hydrochemical characterization of groundwater in wadi Sayyah, Western Saudi Arabia. Appl Water Sci 3:721–732

Al-Charideh A, Abou-Zakhem B, Al-Charideh A, Abou-Zakhem B (2009) Geochemical and isotopic characterization of groundwater from the Paleogene limestone aquifer of the Upper Jezireh, Syria. Environ Earth Sci 59:1065–1078

Ayadi R, Zouari K, Saibi H, Trabelsi R, Khanfir H, Itoi R (2016) Determination of the origins and recharge rates of the Sfax aquifer system (southeastern Tunisia) using isotope tracers. Environ Earth Sci 75:636. https://doi.org/10.1007/s12665-016-5445-4

Bahir M, Mennani A, Jalal M, Youbi N (2000) Contribution à l'étude des ressources hydriques du bassin synclinal d'Essaouira (Maroc). Estudios Geol 56:185–195

Bahir M, Jalal M, Mennani A (2001) Groundwater pollution by nitrates of the Essaouira synclinal basin. J Environ Hydrol 9:18–19

Bahir M, Carreira P, Oliveira da Silva M, Fernandes P (2008) Caractérisation hydrodynamique, hydrochimique et isotopique du système aquifère de Kourimat (Bassin d'Essaouira, Maroc). Estudios Geol 64(1):61–73

Bahir M, Ouhamdouch S, Carreira PM (2016) La ressource en eau au Maroc face aux changements climatiques; cas de la nappe

Plio-Quaternaire du bassin synclinale d'Essaouira. Comun Geol 103(1):35–44

Ben Cheikh N, Zouari K, Abidi B (2014) A hydrogeochemical approach for identifying salinization processes in the Cenomanian–Turonian aquifer, south-eastern Tunisia. Carbonates Evaporites 29(2):193–201

Carreira PM, Marques JM, Nunes D (2014) Source of groundwater salinity in coastline aquifers based on environmental isotopes (Portugal): natural vs. human interference. A review and reinterpretation. Appl Geochem 41:163–175

Clark ID, Fritz P (1997) Environmental isotopes in hydrogeology. CRC Lewis Publishers, New York, p 328

Craig H (1961) Isotopic variation in meteoric water. Science 133:1702–1703

Edmunds WM (2009) Geochemistry's vital contribution to solving water resource problems. Appl Geochem 24:1058–1073

Edmunds WM, Tyler SW (2002) Unsaturated zones as archives of past climates: toward a news proxy for continental regions. J Hydrogeol 10:216–228

Epstein S, Mayeda T (1953) Variation of ^{18}O content of waters from natural sources. Geochim Cosmochim Acta 4:213–224

Ettachfine EM (1992) Le vraconien, Cénomanien et Turonien du bassin d'Essaouira (Haut Atlas Occidental, Maroc). Analyse lithologique, biostratigraphique et sédimentologique, stratigraphie séquentielle. Thèses d'Université, Toulouse, p 245

Farid I, Trabelsi R, Zouari K, Beji R (2013) Geochemical and isotopic study of surface and groundwaters in Ain Bou Mourra basin, central Tunisia. Quat Int 303:210–227

Friedman I (1953) Deuterium content of natural waters and other substances. Geochim Cosmochim Acta 4:89–103

Geyh MA (2000) An overview of ^{14}C analysis in the study of the groundwater. Radiocarbon 42:99–114

Gibbs RJ (1970) Mechanism controlling world water chemistry. Science 170:1088–1090

Giuseppe S, Sibel E, Flavia F (2014) Water quality assessment of carbonate aquifers in southern Latium region, Central Italy: a case study for irrigation and drinking purposes. Appl Water Sci 4:115–128

Gonfiantini R, Zuppi GM (2003) Carbon isotopic exchange rate of DIC in karst groundwater. Chem Geol 197:319–336

Gowrisankar G, Jagadeshan G, Elango L (2017) Managed aquifer recharge by a check dam to improve the quality of fluoride-rich groundwater: a case study from southern India. Environ Monit Assess 189:200. https://doi.org/10.1007/s10661-017-5910-x

Guendouz A, Moulla AS, Edmunds WM, Zouari K, Shand P, Mamou A (2003) Hydrogeochemical and isotopic evolution of water in the complex terminal aquifer in the Algerian Sahara. J Hydrol 11:483–495

IAEA (1976) Procedure and technique critique for tritium enrichment by electrolysis at IAEA Laboratory, Technical Procedure no 19, International Atomic Energy Agency, Vienna

IAEA (1981) Stable isotope hydrology, deuterium and oxygen-18 in the water cycle. Technical report series No 210, IAEA, Vienna

IAEA (1983) Guidebook on nuclear techniques in hydrology. Technical report series Np 91, IAEA, Vienna

Jalal M (2001) Potentialités hydrogéologiques du Cénomano-Turonien du bassin synclinal de Meskala-Kourimat-Ida Ou Zemzem. (Essaouira, Maroc) Thèse de doctorat, Université Cadi Ayyad Maroc, p 192

Kamel S, Hamed Y, Najiba C, Kamel Z (2008) The hydro geochemical characterization of ground waters in Tunisian Chott's region. Environ Geol 54:843–854

Krishna KS, Hari BS, Eswar RP, Selvakumar S, Thivya C, Muralidharan S, Jeyabal G (2017) Evaluation of water quality and hydrogeochemistry of surface and groundwater, Tiruvallur District, Tamil Nadu, India. Appl Water Sci 7:2533–2544

Li C, Ga X, Wang Y (2015) Hydrogeochemistry of high-fluoride groundwater at Yuncheng Basin, northern China. Sci Total Environ 508:155–165

Lozes A (1959) Rapport de synthèse sur les études sismiques dans la zone côtière d'Essaouira, Rapport inédit, Office National de la Recherche Pétrole, Ref. 20048, 25, Rabat

Lucas LL, Unterweger MP (2000) Comprehensive review and critical evaluation of the half-life of tritium. J Res Natl Inst Technol 105:541–549

Mazor E (1991) Applied chemical and isotopic groundwater hydrology. Open University Press, Buckingham

Mennani A (2001) Apport de l'hydrochimie et de l'isotopie à la connaissance du fonctionnement des aquifères de la zone côtière d'Essaouira (Maroc Occidental). Thèse de doctorat, Université Cadi Ayyad Maroc, p 152

Nagaraju A, Sunil Kumar K, Thejaswi A (2014) Assessment of groundwater quality for irrigation: a case study from Bandalamottu lead mining area, Guntur District, Andhra Pradesh, South India. Appl Water Sci 4:385–396

Ouhamdouch S, Bahir M (2017) Climate change impact on future rainfall and temperature in semi-arid areas (Essaouira Basin, Morocco). Environ Process 4(4):975–990

Ouhamdouch S, Bahir M, Carreira P, Chkir N, Goumih A, Chamchati H (2016a) Climate change impact on aquifer system of Essaouira basin during the past 4 decades (Morocco). Open J Mod Hydrol 6:19–33

Ouhamdouch S, Bahir M, Carreira P, Chkir N, Goumih A (2016b) Impact du changement climatique sur l'aquifère Hauterivien bu bassin d'Essaouira (Maroc). Larhyss J 25:269–283

Ouhamdouch S, Bahira M, Carreira PM (2017) Geochemical and isotopic tools to deciphering the origin of mineralization of the coastal aquifer of Essaouira basin, Morocco. Procedia Earth Planet Sci 17:73–76

Ouhamdouch S, Bahir M, Ait-Tahar M, Goumih A, Rouissa A (2018) Physico-chemical quality and origin of groundwater of an aquifer under semi-arid climate. Case of the Barremo-Aptian aquifer of Essaouira basin (Morocco Occidental). J Mater Environ Sci 9(3):1022–1034

Parkhurst DL, Appelo CAJ (1999) User's guide to PHREEQC (version 2): a computer program for speciation, batch reaction, one dimensional transport, and inverse geochemical calculations. US Geol Surv Water Resour Invest Rep 99(4259):4312

Piper AM (1944) A graphic procedure in the geochemical interpretation of water analyses. Trans Am Geophys Union 25:914–923

Qin R, Wua Y, Xu Z, Xie D, Zhang C (2013) Assessing the impact of natural and anthropogenic activities on groundwater quality in coastal alluvial aquifers of the lower Liaohe River Plain, NE China. Appl Geochem 31:142–158

Re V, Sacchi E, Martin-Bordes JL, Aureli A, El Hamouti N, Bouchnan R, Zuppi GM (2013) Processes affecting groundwater quality in arid zones: the case of the Bou-Areg coastal aquifer (North Morocco). Appl Geochem 34:181–198

Tijani MN, Loehnert EP, Uma KO (1996) Origin of saline groundwaters in the Ogoja area, Lower Benue Trough, Nigeria. J Afr Earth Sci 23:237–252

USSL (1954) Diagnosis and improvement of saline and alkaline soils. United States Salinity Laboratory, US Department of Agriculture, Washington

Vitvar T, Aggarwal PK, McDonnell JJ (2005) A review of isotope applications in catchment hydrology. In: Aggarwal PK, Gat J, Froehlich KFO (eds) Isotopes in the water cycle: past, present and future of a developing science. Springer, Berlin, pp 151–170

Wilcox LV (1955) Classification and use of irrigation waters. USDA Circ. 969, Washington, DC

World Health Organization WHO (2008) Guidelines for drinking water quality, 3rd edn. p 494. ISBN 978 92 4 154761 1

مدينة الملك عبدالعزيز
KACST للعلوم والتقنية

Springer